GLOBAL THERMAL INERTIA AND SURFACE ROUGHNESS OF ASTEROID 162173 RYUGU BY TIR ON HAYABUSA2. Y. Shimaki[1], H. Senshu[2], N. Sakatani[1], T. Okada[1], T. Fukuhara[3], S. Tanaka[1], T. Arai[4], H. Demura[5], K. Suko[5], T. Sekiguchi[6], T. Kouyama[7], J. Takita[8], M. Taguchi[3], and S. Hasegawa[1], [1]Institute of Space and Astronautical Science, Japan Aerospace Exploration Agency (3-1-1 Yoshinodai, Chuo, Sagamihara, Kanagawa 252-5210, Japan, shimaki@plaenta.sci.isas.jaxa.jp). [2]Chiba Institute of Technology, Japan. [3]Rikkyo University, Japan. [4]Ashikaga University, Japan. [5]University of Aizu, Japan. [6]Hokkaido University of Education, Japan. [7]National Institute of Advanced Industrial Science and Technology, Japan. [8]Hokkaido Kitami Hokuto High School, Japan.

Introduction: The thermal infrared imager TIR has been acquired thermal images of the C-type near-Earth asteroid 162173 Ryugu since June 2018. Observations for one asteroid rotation from a spacecraft position, such as the Home Position located at the 20 km altitude of sub-Earth point, enable us to trace apparent diurnal temperature change of a surface of Ryugu. The temperature profiles of Ryugu show flat pattern ubiquitously, which indicates strong effects of surface roughness, and the global thermal inertia is estimated to be around 200-300 J m^{-2} K^{-1} $s^{-0.5}$ (=tiu) [1,2]. The value is consistent with the ground observations [3] and the in-situ measurements by MARA on MASCOT [4] but is less than the value of Bennu [5]. In this study, we examined global thermal properties including surface roughness of Ryugu by comparing TIR observations and thermophysical model (TPM) calculations.

Methods: *TIR observations.* TIR is based on a two-dimensional uncooled bolometer array inherited from the Akatsuki Venus Orbiter [6]. The thermal images are converted to the brightness temperature images via the calibration curves based on the pre-flight ground tests, and those brightness temperature images are projected onto a shape model of Ryugu using SPICE kernels [7]. A shape model of Ryugu composed of 200k polygon with a spatial resolution of ~2 m/polygon (SHAPE_SFM_200k_v20180804) was used [8]. With an observation for one-asteroid rotation, a diurnal temperature profile of a facet of the shape model was obtained. We used 112 out of 120 thermal images obtained at the Mid altitude operation on August 1, 2018, with one of the highest resolution (~4.5 m/pixel). During the observation, the solar-spacecraft-earth angle was ~20˚, the sub-solar latitude was -8.4˚, and the heliocentric distance of Ryugu was 1.06 AU. We assumed the emissivity of 0.95 instead of nominal value of 1.0.

TPM calculations. Two TPMs are used to evaluate results of TIR. One is a TPM using a shape model of Ryugu (TPM1) based on [9] and the other is one using a fractal rough surface (TPM2) based on [10]. We applied similar parameters, such as rotation axis and heliocentric distance, for both calculations. Emissivity of 0.95 was assumed. Albedo of 0.045 (bond albedo [11]) for TPM1 and 0.0146 (geometric albedo [2]) for TPM2 were assumed. For TPM1, we varied the thermal inertia γ from 20 to 800 tiu. For TPM2, we varied the latitude of the fractal rough surface from -88˚N to 88˚N, the thermal inertia from 10 to 800 tiu, and the surface roughness from 0 (flat) to 0.5 (rough).

Estimation of thermal inertia. The thermal inertia of a position of Ryugu is estimated from the maximum temperature by TPM1 and from the pattern of diurnal temperature profile by TPM2. The method using TPM1 is a similar one used in the landing site selection (LSS) for the first touchdown [12]. On TPM2, we used 4-order function to characterize diurnal temperature profiles at local time from 10 to 16 hour. From the regression analysis of the fitting coefficients of temperature profiles by TPM2, we obtained empirical equations to estimate thermal inertia and surface roughness from the fitting coefficients. We applied surface tilt angle correction in ±15˚ both in longitude and latitude, since a shape model reduces surface slope due to limitation of resolution. We regulate analysis on the dataset with the solar incident angle <35˚.

Results and Discussions: *Thermal inertia of Ryugu using TPM1.* TPM1 provides a temperature profile of a surface of a shape model of Ryugu [7,13] and the temperatures reached maximum at low latitudes, since the solar incident angle defines input solar flux. As a result, the thermal inertia of Ryugu estimated by TPM1 shows latitudinal variation with a peak at the equatorial ridge with ~400 tiu, with the global mean of 280±140 tiu. No thermal inertia was obtained at high latitudes, because no TPM1 calculation reproduced observed maximum temperature. Although the global thermal inertia is in the range of the values by the ground and the in-situ observations [3,4], no geologic variation in latitude was observed by the optical navigation camera (ONC) [2]. Thus, we consider that this global thermal inertia is useful only for a prediction of maximum temperature for given epoch required in the LSS.

Thermal inertia of Ryugu using TPM2. TPM2 gives flat temperature profile as a function of a thermal inertia, a surface roughness, and a latitude of rough surface. Regression equations for thermal inertia and surface roughness for each latitude were obtained. Using the 4-order fitting coefficients of an observed

temperature profile of a facet, the thermal inertia and the surface roughness of the facet was obtained.

Figure 1 shows the map of the thermal inertia with variations in the longitude and the latitude. Locations of natural craters are shown by circles. The thermal inertia of Ryugu shows homogeneous distribution both in the longitude and latitude, with the global thermal inertia of 210±50 tiu. We could not determine the thermal inertia at high latitudes.

The surface roughness map of Ryugu by TPM2 is shown in Figure 2. Similar to the thermal inertia map, the surface roughness shows homogeneous distribution with the mean value of 0.42±0.02, corresponds to moderately rough surface. The relatively low thermal inertia and the high surface roughness suggests that the surface of Ryugu is covered by numerous boulders with low thermal inertia.

We investigated the thermal inertia of natural craters and found no dependence of the thermal inertia on crater size, suggesting that there is no compaction craters. Besides inside of the craters, ejecta depositions surrounding these craters were not observed in the thermal inertia map. The lower global thermal inertia of Ryugu might be results from porous and probably fragile nature of C-type asteroid as an ancestor of carbonaceous chondrites.

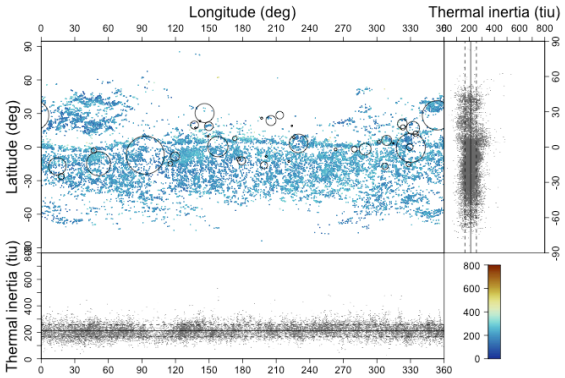

Figure 1. Thermal inertia map with latitudinal and longitudinal variations. Natural craters are shown by circles.

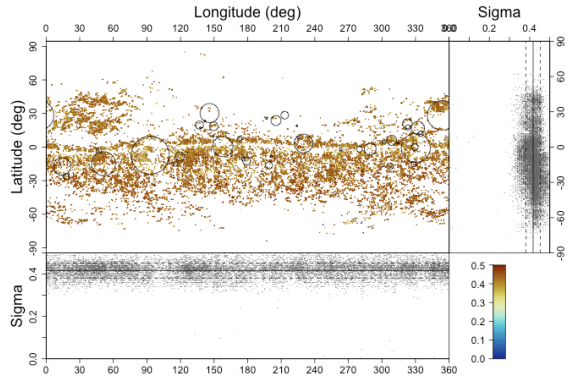

Figure 2. Surface roughness (sigma) map with latitudinal and longitudinal variations.

Acknowledgments: The authors would express thanks to the Hayabusa2 team members for their technical and operational supports and for helpful scientific discussions. This study is supported by the JSPS KAKENHI No. J17H06459 (Aqua Planetology).

References: [1] Okada T. et al. (2019) *LPSC 50th*, #1325. [2] Sugita S. et al. (2019) *Science*, 364(6437), eaaw0422. [3] Müller T.G. et al. (2017) *A&A*, 599:A103. [4] Grott M. et al. (2019) *Nature Ast*. doi: 10.1038/s41550-019-0832-x. [5] D. N. DellaGiustina et al. (2019) *Nature Ast*. Doi:10.1038/s41550-019-0731-1. [6] Fukuhara T. et al. (2011) *EPS*, 63:1009–1018. [7] Arai T. et al. (2019), *This conference*. [8] Watanabe S. et al. (2019) *Science*, 364(6437), 268–272. [9] Takita J. et al. (2017) *SSR*, 208(1- 4):287–315. [10] Senshu H. et al. (2019) *LPSC 50th*, #2153. [11] Ishiguro M. et al. (2014) *ApJ*, 792(1):74 [12] Yabuta H. et al. (2019) *LPSC 50th*, #2304. [13] Tanaka S. et al. (2019) *This conference*.